Lasers in Manufacturing Conference 2019

Ultrafast Laser Ablation of Transparent Ceramics: The Role of the Pulse Duration on the Ablation Mechanisms

C. Kalupka[a*], M. Schmalstieg[b]

[a]*Fraunhofer Institute for Laser Technology ILT, Steinbachstraße 15, 52074 Aachen, Germany*
[b]*Chair for Laser Technology LLT, RWTH Aachen University, Steinbachstraße 15, 52074 Aachen, Germany*

Abstract

In recent years, novel transparent ceramics have been developed which combine advantages of high mechanical strength and thermal capacity with optical transparency and a high refractive index. For this new material class, conventional processing is a major challenge in particular due to the hardness, therefore ultrashort pulse processing is a promising technique for high precision and efficient machining of the transparent ceramics. In this study, we report on the surface laser ablation of three different ceramics – spinel $MgAl_2O_4$, aluminum oxide Al_2O_3, zirconium oxide ZrO_2 – with ultrashort laser pulses. In particular, we vary the pulse energy and the pulse duration from 100 fs up to 10 ps to investigate the impact of temporal intensity distribution on the ablation mechanism and result. We combine ex situ investigations of the processed areas with in situ ultrafast pump probe microscopy therefore enabling an extensive study of the underlying ablation mechanisms.

Keywords: ultrashort pulse processing ; transparent ceramics ; surface ablation ; pulse duration ; ablation mechanisms

1. Introduction

The demands on novel transparent materials with optimized optical, mechanical and thermal properties have increased over recent years for example in the field of transparent armor applications [Krell et al, 2008]. Moreover, transparent materials with a high refractive index and high thermal and mechanical stability exhibit promising potential for fields of consumer electronics or optical applications. Ceramics have

* Corresponding author. Tel.: +49 241 8906 276; fax: +49 241 8906 121.
E-mail address: christian.kalupka@ilt.fraunhofer.de .

several advantages compared to glasses for example the high thermal capacity and high mechanical strength. Typically ceramics show low transparency as a consequence of porosity, large grain sizes in the order of µm and birefringence. Novel polycrystalline ceramics have been developed which exhibit a high real inline transmission, for example for spinel $MgAl_2O_4$ up to 87% at 600 nm [Krell et al, 2010] [Goldstein et al, 2016], thus enabling a wide range of applications for transparent ceramics.

The unique properties of transparent ceramics lead to the demand on a promising processing technology. Due to the hardness in the order 1500HV10, conventional mechanical processing leads to severe degeneration of the tools and a long process duration [Goldstein et al, 2016] [Klocke et al, 2018]. Moreover the spatial precision and flexibility is hard to achieve. Here, ultrashort pulsed laser ablation is a promising technology to overcome the challenges since a contactless, fast and precise processing is possible. First results have been published recently [Kalupka and Schmalstieg et al, 2018]. To enable a technology for processing transparent ceramics, the underlying ablation mechanisms for this novel class of materials must be understood. We use three different ceramics, $MgAl_2O_4$, ZrO_2 and Al_2O_3, with different mechanical, optical and thermal properties. A selection of properties is presented in Table 1. All ceramics are developed and produced by the Fraunhofer Institute for Ceramic Technologies and Systems (IKTS) in Dresden, Germany.

Table 1. Selection of properties of the used transparent ceramics in this study.

	$MgAl_2O_4$	ZrO_2	Al_2O_3
Grain size	0.6 µm	180 µm	0.5 µm
Hardness	1464HV10	1354HV10	2095HV10
Young's modulus	274 GPa	215 GPa	399 GPa

In this study, we report on fundamental aspects of ultrashort pulsed laser ablation of transparent ceramics by an investigation of the underlying ablation mechanisms in dependency on the applied pulse parameters. To investigate the impact of energy input on the ablation mechanisms, we vary the pulse duration from 0.1 to 10 ps. In general, short pulse durations can lead to, so-called, non-thermal ablation mechanisms since a heating of the lattice by the pulse is less pronounced. For longer the pulse durations in the order of several ps, thermal ablation mechanisms might dominate due to the longer heating of the lattice [Chichkov et al, 1996]. Therefore, different dynamics of the generated free electrons and the lattice can result in dependency on the applied pulse duration. Thus, we perform in situ measurements of the reflectivity of the irradiated ceramic surfaces by time-resolved pump probe microscopy since the generation of free electrons and heating of the lattice change the optical properties of the ceramic surface [Kalupka and Holtum et al, 2018]. On the one hand side, we focus on a time scale < 20 ps to investigate the generation and relaxation dynamics of free electrons as a consequence of optical energy input. On the second hand side, we perform measurements up to 1.5 ns to image the ablation dynamics.

2. Experimental setup

We use a Ti:Sapphire chirped pulse amplification laser source ("Libra", Coherent) to perform single pulse ablation experiments of the ceramics. The laser source emits linear polarized pulses with a central wavelength of 800 nm with a pulse energy of 2 mJ. The pulse duration can be adjusted in a range from 80 fs to 10 ps (full width half maximum for a temporal Gaussian beam shape) and the pulse energy is set by the combination of a half-wave plate and a thin film polarizer. The pulses are focused on the surface of the ceramic with a plano-convex lens with focal length of 150 mm resulting in a focus spot diameter of 30 µm.

The ceramic samples are translated after each ablation experiment by a linear stage, so an unmodified surface is irradiated for a subsequent ablation to avoid incubation effects.

For in situ reflection measurements, we use the same laser source in a pump probe setup. Here, a single pulse with a pulse duration of 100 fs is split into a pump and a probe pulse by a beam splitter. The pulse duration of the pump pulse can be adjusted by a pulse stretcher based on a two-pass reflection grating setup. Therefore, the probe pulse duration remains unchanged enabling a temporal resolution of 100 fs. The pump pulse is focused onto the sample surface with the same plano-convex lens with an incident angle of approximately 43°, so an elliptical beam profile results on the surface. The relative delay between pump and probe pulse can be adjusted by changing the probe propagation distance with a variable linear stage up to 1.5 ns. The probe pulse is frequency doubled by a Beta Barium Borat crystal to 400 nm and guided to the sample surface by a microscope objective (20x, NA 0.4). The reflected probe intensity is focused onto the chip of a CMOS camera with a plano-convex lens with a focal length of 150 mm resulting in a spatial resolution of approximately 1 µm. In front of the CMOS chip, a band pass filter for 400 nm is mounted to avoid the influence of room light and intense plasma emission. Before an image with the pump pulse is recorded, a background image is acquired to calculate the normalized reflected intensity of the probe pulse for each pixel.

For the experiments, we use three different ceramics $MgAl_2O_4$, ZrO_2 and Al_2O_3, see Table 1. The surfaces of the ceramics are mechanically grinded and polished to a surface roughness < 0.5 µm. The ceramics are mounted onto a movable translation stage.

3. Results

3.1. Ablation of ceramics: Role of fluence and pulse duration

By performing single pulse ablation experiments on the surface of the selected ceramics, evidence of the dominant ablation mechanisms can be identified by optical microscopy of the ablation craters. The underlying ablation mechanisms strongly depend on the overall optical energy input in the sample. For ultrashort laser pulses, the energy input is correlated with the temporal intensity distribution, which is determined by the pulse duration as well as the peak intensity for a known temporal beam profile. In addition, the energy input is also strongly dependent on the transient optical properties of the sample. Therefore, a complex interplay of temporal intensity distribution and transient material properties results. In order to keep the number of varied parameters to a minimum, in a first step the pulse duration is kept constant and the peak intensity is varied by changing the applied fluence F or pulse energy, respectively.

Figure 1 (a) shows surface ablation craters on spinel $MgAl_2O_4$ for a pulse duration of 1 ps and fluences F from 3 to 25 J/cm². For F ≤ 7 J/cm², the ablation crater exhibits evenly distributed dark features. Exceeding a fluence of 8 J/cm², an additional feature evolves in the center of the ablation crater, which appears to have a smoother surface compared to the dark features. An increase of fluence up to 25 J/cm² leads to an ablation crater with almost only the smooth surface. The occurrence of the different ablation features can be explained by different dominant ablation mechanisms, which depend on the applied fluence. Here, we propose that the smooth feature is a result of an ablation dominated by melting and vaporization for high fluences, whereas the dark features might occur due to spallation leading to a higher surface roughness which is dominant for lower fluences.

To change the local energy input, we vary the pulse duration from 0.1 up to 10 ps. The fluence is kept constant to 27 J/cm² to observe all potential ablation features compared to Figure 1 (a). As a consequence of the variation of the pulse duration, the laser intensity is varied by almost two orders of magnitude.

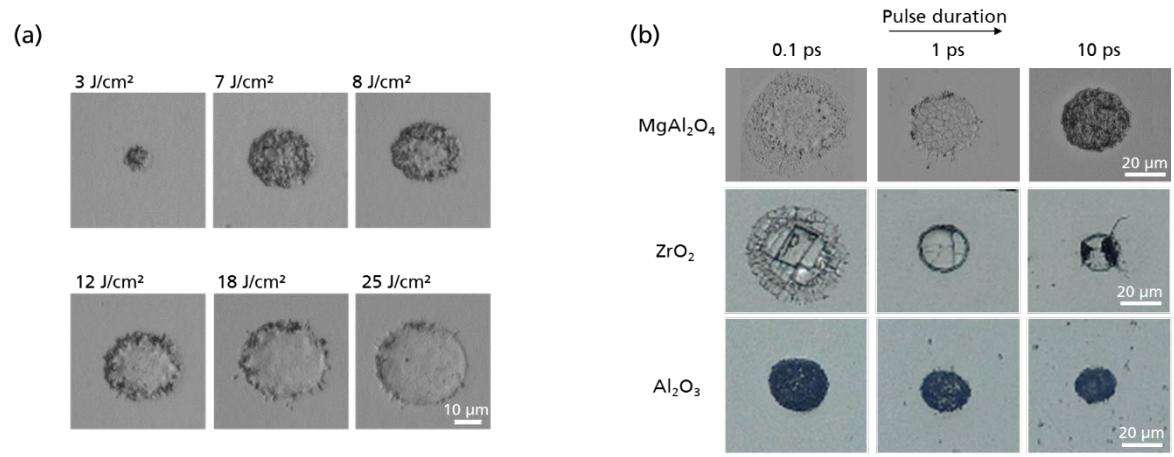

Fig. 1. (a) Surface ablation craters on spinel $MgAl_2O_4$ generated by single pulses with a pulse duration of 1 ps for a variation of applied fluence; (b) surface ablation craters on three ceramics for pulse durations 0.1, 1 and 10 ps for a fluence of 27 J/cm².

For all three ceramics, the diameters of the ablation craters decrease for an increase of the pulse duration, which indicates a higher ablation threshold in terms of fluence.

The ablation crater of $MgAl_2O_4$ exhibits for the pulse duration 0.1 ps a smooth surface profile as described in Figure 1 (a) and in addition melt features are observed. This reveals that for high intensities, ablation by melting is a pronounced ablation mechanism. For the pulse duration 1 ps, we detect additional crack-like features in the center of the ablation crater as a consequence of the higher fluence F = 27 J/cm² compared to Figure 1 (a). The crack length is in the order of approximately 5 µm, therefore a correlation with the average grain size of 0.57 µm is unlikely. For the longest pulse duration of 10 ps, only dark ablation features occur.

For ZrO_2, two ablation regimes are detected for 0.1 ps, which corresponds to different fluence thresholds for the ablation mechanisms. The inner area of the ablation crater exhibits straight lines for 0.1 and 1 ps. In fact, the morphology indicates strong spallation and the formation of cracks as dominant mechanism. For the pulse duration 10 ps, holes evolve and large cracks are identified. This might indicate a pronounced spallation process of material, which ablates much larger clusters of material compared to melting or vaporization. We suggest that the formation of large cracks and spallation of material is correlated to the comparable large grain size 180 µm of the used ZrO_2.

In contrast to $MgAl_2O_4$ and ZrO_2, only one ablation regime is identified for Al_2O_3 by a homogenously dark ablation crater. The morphology of the ablation crater remains constant for a variation of the pulse duration from 0.1 to 10 ps. The overall morphology is comparable to the ablation crater on $MgAl_2O_4$ for a pulse duration of 10 ps. Therefore we conclude that the underlying ablation mechanisms are comparable.

3.2. In situ measurements of transient reflectivity

In order to investigate potential physical origins of the observed ablation features in the previous section, we perform in situ measurements of the transient material properties by means of time-resolved pump-probe microscopy. In particular, measurements of the surface reflectivity reveals features of initial free electron generation as a consequence of optical energy deposition on a time scale up to several ten picoseconds. Moreover, ablation processes like removal of vaporized material and shock wave propagation take place on a time scale > 100 ps up to several nanoseconds or even microseconds.

In Figure 2 the transient reflectivity of the probe pulse of all three ceramic surfaces is shown for a fluence of F = 4 J/cm² for different time delays between pump and probe pulse up to approximately 1.5 ns. The images are normalized to the intrinsic reflectivity of each ceramic surface. The pump pulse duration is kept constant to 0.1 ps to investigate all features observed in Figure 1 (b).

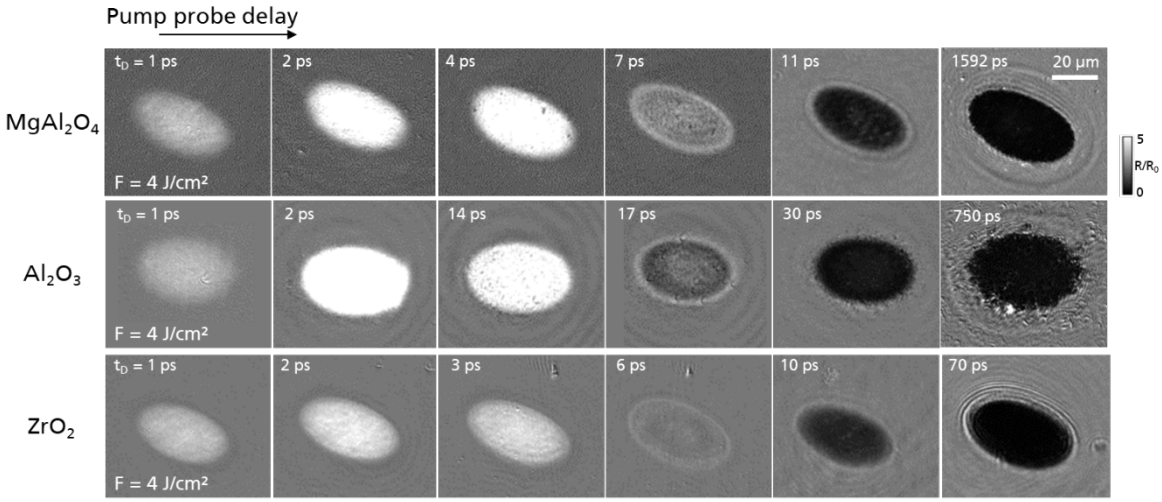

Fig. 2. Transient reflectivity of irradiated ceramic surfaces with a single pump pulse with a pulse duration of 100 fs and a fluence of 4 J/cm² for different times t_D after irradiation measured by time-resolved pump probe microscopy. The reflectivity R is normalized to the intrinsic reflectivity R_0 of each ceramic.

For all ceramics, the reflectivity strongly increases within the first approximately 6 ps after initial excitation. This corresponds to the laser-induced excitation of free electrons by multiphoton and subsequent avalanche ionization. Since the pump pulse duration is 100 fs, the intrinsic impact ionization time of the ceramics exceeds the femtosecond regime. Moreover, the relaxation time of the free electrons appears to be in the same order of magnitude. Therefore, the dense free electron plasma is observed up to several ps after initial excitation. A ring structure on the outside region of the irradiated are is detected for all three ceramics at approximately 6 to 7 ps. This reveals that excitation dynamics depend on the applied fluence. The fluence in the outer area is close to the specific ablation threshold. Therefore the free carrier dynamics are slower for fluences near the ablation threshold. For a time scale exceeding approximately 10 ps, the reflectivity of the irradiated area strongly decreases. This is typically explained by a strong heating of the lattice and an onset of ablation. The low reflectivity remains constant up to the nanosecond regime. Additionally an axial shock wave is observed which indicates ablation of vaporized material. For Al_2O_3, particle-like features are observed at 750 ps in the outer region of the irradiated area. Overall, comparable characteristic features observed in the ex situ analysis of surface ablation craters in Figure 1 (a) and (b) are not observed by in situ measurements. Therefore, we conclude that the processes leading to such features occur on a timescale exceeding 1.5 ns.

To investigate the impact of the temporal intensity distribution on the ablation dynamics, we increase the pump pulse duration to approximately 10 ps. In Figure 3, the reflection of the probe beam of a spinel $MgAl_2O_4$ surface is shown for a fluence of F = 8 J/cm² for time delays up to 750 ps after initial excitation.

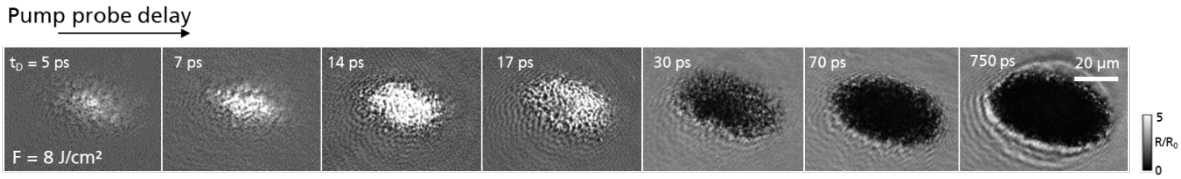

Fig. 3. Transient reflectivity of a irradiated spinel $MgAl_2O_4$ surface with a single pump pulse with a pulse duration of 10 ps and a fluence of 8 J/cm² for different times t_D after irradiation measured by time-resolved pump probe microscopy. The reflectivity R is normalized to the intrinsic reflectivity R_0 of the ceramic.

In the first 17 ps after initial excitation, the reflectivity of the spinel surface increases, which is in accordance to the irradiation with a pump pulse duration 100 fs. Analogously, this is explained by the generation of a free electron plasma. Here, the overall excitation process lasts longer compared to 100 fs since the pulse duration is 10 ps and therefore the generation of free electrons is in the same order of magnitude. In contrast to Figure 2, the irradiated area exhibits diffuse and sparkled features. Some dark spots are identified in the irradiated area at approximately 17 ps which indicates the onset of formation of ablation products. After 30 ps up to 750 ps, the reflectivity strongly decreases and the formation of a shock wave is observed. Overall, the general temporal evolution of the reflectivity is comparable to the use of a pump pulse duration of 100 fs. For the pulse duration 10 ps, the diffuse dark features observed after 17 ps can be correlated to features of the ablation crater for spinel for the pulse duration 10 ps in Figure 1. Thus the ablation mechanisms for spinel sets in approximately 17 ps after initial excitation of the free electron plasma. The qualitatively comparison of ex and in situ analysis methods reveal that the evolution of ablation features can be identified by means of in situ measurements.

4. Conclusion

In summary, we have presented a principle investigation of ultrashort pulsed laser ablation of three different transparent ceramics $MgAl_2O_4$, ZrO_2 and Al_2O_3. For a variation of the pulse durations from 0.1 to 10 ps different ablation regimes are identified as a function of the applied fluence. For 0.1 ps the ablation craters reveal a melt dominated ablation mechanism for $MgAl_2O_4$ and ZrO_2, which can originate from the applied high peak intensities due to the short pulse duration. For ZrO_2 strong spallation is observed for a pulse duration exceeding 1 ps which is correlated to the relatively high grain size compared to the other ceramics. In situ measurements of the transient reflectivity reveal comparable excitation and relaxation dynamics of free electrons for all ceramics. Moreover, we find evidence for the ablation of vaporized material and particles in particular for a pulse duration of 10 ps. By additional in situ measurements on a time scale exceeding 1.5 ns, the formation of ablation products and the ablation dynamics will be investigated in more detail. Moreover, in situ measurements are planned for a much wider range of processing parameters.

Acknowledgements

This work was supported by the Fraunhofer Internal Programs under Grant No. MAVO 833 916.

References

Chichkov, B. N., Momma, C., Nolte, S., Von Alvensleben, F., & Tünnermann, A. (1996). Femtosecond, picosecond and nanosecond laser ablation of solids. *Applied Physics A*, *63*(2), 109-115.

Goldstein, A., & Krell, A. (2016). Transparent ceramics at 50: progress made and further prospects. *Journal of the American Ceramic Society*, *99*(10), 3173-3197.

Kalupka, C., Schmalstieg, M., & Reininghaus, M. (2018). Ultrashort Pulse Processing of Transparent Ceramics: The Role of Electronic and Thermal Damage Mechanisms. *Journal of Laser Micro/Nanoengineering*, *13*(2).

Kalupka, C., Holtum, T., & Reininghaus, M. (2018, February). Ultrafast dynamics of material excitation of dielectrics with ultrashort pulsed Bessel beams. In *Laser-based Micro-and Nanoprocessing XII* (Vol. 10520, p. 105200G). International Society for Optics and Photonics.

Klocke, F., Dambon, O., Bletek, T., Höche, T., Naumann, F., & Hutzler, T. (2018). Surface Integrity in Ultra-Precision Grinding of Transparent Ceramics. *Procedia CIRP*, *71*, 177-180.

Krell, A., Klimke, J., & Hutzler, T. (2009). Advanced spinel and sub-µm Al2O3 for transparent armour applications. *Journal of the European Ceramic Society*, *29*(2), 275-281.

Krell, A., Hutzler, T., Klimke, J., & Potthoff, A. (2010). Fine-grained transparent spinel windows by the processing of different nanopowders. *Journal of the American Ceramic Society*, *93*(9), 2656-2666.